



RESEARCH ARTICLE

Transient thrust behavior of low-aspect-ratio rocket propulsion systems

Aref Zanjani | Amir Mahdi Tahsini 

School of Mechanical Engineering, Iran
University of Science and Technology,
Tehran, Iran

Correspondence

Amir Mahdi Tahsini, School of
Mechanical Engineering, Iran University
of Science and Technology, 1684613114
Tehran, Iran.
Email: am_tahsini@iust.ac.ir

Abstract

In this work, the transient thrust force of the solid propellant rocket motor is numerically computed to illustrate the shortcomings of the common thrust formula in transient periods of operation. The internal ballistics of the solid rocket motor is simulated using the quasi one-dimensional governing equations in which the finite volume method and the Roe's scheme are utilized in calculation procedure. This is demonstrated that in transient operation of the propulsion systems, the common thrust formula may ignore some parts of physical phenomena because it has been derived based on steady state assumption, but there are some moving waves in transient operation in the combustion chamber which induce the fluctuations on the thrust force. So, the thrust-time history must be computed by pressure force integration over the whole solid boundaries of the motor at any instant. The results show that such transient thrust behavior is more intense in low aspect ratio propulsion systems like small space thrusters.

KEYWORDS

numerical study, propulsion, rocket, solid propellant, thrust, transient

1 | INTRODUCTION

Transient behavior of a complicated system is not often easy to predict because it is very time consuming especially if the physical time of the process is considerably long. So the unsteady problems are usually analyzed using the quasi-steady simulations with lower computational times [1]. On the other hand, the quasi-steady simulations are based on some simplifying assumptions which sometimes may decrease the accuracy of results.

This issue is more acute when the problem has diverse phenomena with different time scales. In such

situations, the use of the quasi-steady method will lead to ignoring some parts of physics and a significant error in the prediction [2, 3]. In addition, the unsteady simulations are sometimes accurate, but to evaluate a performance parameter, a formula may be used that is derived based on steady state conditions. Therefore, although the main problem is computed properly, some outputs may be inaccurate or even incorrect.

A good example is predicting the performance of propulsion systems which is important to anticipate the flight trajectory of the vehicle or any other expected functionality. Even if the performance is steady in most

A, flow port area [m²]; a , pressure coefficient of the burning rate model; A_b , burning area [m²]; A_e , nozzle exit area [m²]; c_p , gas specific heat [J/kgK]; E , total specific internal energy [J/kg]; F_c , thrust force calculated by common formula [N]; F_r , real thrust force, calculated by pressure force integration [N]; \dot{m} , nozzle exit mass flow rate [kg/s]; n , pressure exponent of the burning rate model; p , pressure [Pa]; p_a , ambient pressure [Pa]; p_e , nozzle exit pressure [Pa]; r , propellant burning rate [m/s]; t , time [s]; T , temperature [K]; u , axial velocity [m/s]; u_e , nozzle exit velocity in x direction [m/s]; V_f , gas injection velocity at the propellant surface [m/s]; x , axial coordinate [m]; ρ , gas density [kg/m³]; ρ_p , propellant density [kg/m³]

of the operational time, turning the propulsion system on and off are completely transient processes. So, depending on the required accuracy for transient performance prediction of the system, the quasi-steady or the unsteady method can be utilized to solve the governing equations inside the flow field. Then, the most important performance parameter of the engine, the thrust force, can be computed. But it should be emphasized that in most of the performed transient studies, the transient thrust force of the system is computed by the general thrust formula using the nozzle exit momentum and pressure.

Whitmore et al. [4] presented a novel technique to reconstruct high-frequency chamber pressure measurements in transient situations in which their analysis on the thrust force was based on the general thrust formula. Drummond [5] focused on transient thrust prediction for an ejector propulsion system using common thrust force formula too. Whitmore and Chandler [6] developed a transient thrust model for hybrid rocket motor where they just focused on transient behavior of the flow field. Ponti et al. [7] developed an unsteady simulation tool for internal ballistics studies still without any attention to the transient thrust behavior accurately. Although Song et al. [8] focused on calculating the transient flow characteristics within a solid rocket motor having a pintle nozzle, which has highly unsteady features, they used a common thrust force formula based on exit momentum and pressure in their studies, too. Other researches have been done in the field of transient phenomena in rocket engines [9–13].

In the present study, the accurate prediction of the transient thrust force of the solid rocket motor is performed to evaluate the shortcomings of the common thrust formula and investigate the importance of such consideration if the difference is significant.

2 | GOVERNING EQUATIONS AND NUMERICAL PROCEDURE

To study the transient thrust behavior of the propulsion system accurately, the solid propellant rocket motor with internal burning cylindrical grain is under consideration here. So the quasi-one-dimensional governing equations for the compressible flow including the mass, axial momentum, and energy equations are used which are presented in the conservation form as [14]:

$$\frac{\partial Q}{\partial t} + \frac{\partial G}{\partial x} = S \quad (1)$$

$$Q = \begin{bmatrix} \rho A \\ \rho u A \\ \rho E A \end{bmatrix} \quad G = \begin{bmatrix} \rho u A \\ (\rho u^2 + p) A \\ \rho u H A \end{bmatrix} \quad (2)$$

$$S = \begin{bmatrix} S_m \\ p \frac{dA}{dx} \\ S_m \left(c_p T_f + \frac{1}{2} V_f^2 \right) \end{bmatrix}$$

Where,

$$H = E + \frac{p}{\rho} \quad (3)$$

$$E = c_v T + \frac{u^2}{2}$$

$$S_m = \frac{1}{\Delta x} \frac{dm}{dt} \quad (4)$$

$$\frac{dm}{dt} = \rho_p r A_b$$

$$V_f = \frac{\rho_p}{\rho} r$$

$$r = ap^n$$

Here ρ is density, p is pressure, T is temperature, H is total specific enthalpy, E is total specific internal energy, c_p is the combustion gas specific heat at constant pressure, u is the axial velocity, A is the flow port area, S_m is the combustion gas mass generation rate per unit length of burning surface of the propellant grain, T_f is the flame temperature, V_f is the injection velocity at the propellant surface, ρ_p is the propellant density, A_b is the propellant burning area, and r is the propellant burning rate which is computed by simple pressure dependent model where a is the coefficient and n is the pressure exponent. The source terms of the mass and energy equations are the result of the propellant burning which enters the hot gas into the flow field.

The spatial discretization of these governing equations is performed by using a finite volume method where the information of the flow field is stored at the center of the computational cells. To implement this

method, the conservation equations are integrated first along the cell:

$$\begin{aligned} \int_x \left(\frac{\partial Q}{\partial t} + \frac{\partial G}{\partial x} = S \right) dx \\ \int_x \frac{\partial Q}{\partial t} dx + \int_x \frac{\partial G}{\partial x} dx = \int_x S dx \quad (5) \\ Q^{n+1} = Q^n + \frac{\Delta t}{\Delta x} \left(G_{i+\frac{1}{2}} - G_{i-\frac{1}{2}} \right) + S \Delta t \end{aligned}$$

Then, the convective flux on each face of the cells is calculated by applying the upwind Roe's scheme [15]. Appropriate boundary conditions are applied at the nozzle exit according to the instantaneous flow Mach number. At the non-burning head-end, a wall boundary condition is applied. For time discretization, an explicit method is employed when the fluxes are integrated over each control surface. Similar time step is used for all cells at any iteration to obtain the physical transient result for the flow field. The real time-span of the studies is so short that the regression of the burning surface could be ignored; therefore the geometry of the flow field has no change during the computations. More details about computing procedure and validations have been presented in Ref. [16–18].

By simulating the flow field at any instant, the thrust force of this propulsion system could be calculated at that time, so the thrust-time history which is the most important performance curve of the engine is finally achieved. The focus here is how to compute the thrust force. This has been always done using common thrust force formula as:

$$F = \dot{m} u_e + (p_e - p_a) A_e \quad (6)$$

Where F denotes the thrust force, and \dot{m} , u_e , p_e , p_a , and A_e are the exhaust mass flow rate, exit velocity, exit pressure, ambient pressure, and nozzle exit area respectively. But this formula is obtained by applying the momentum equation to the proper control volume around the engine at steady condition, which helps to compute easily the thrust force based on the nozzle exit momentum and pressure, instead of integrating the pressure force over the combustion chamber and nozzle walls.

But at an unsteady condition, this formula cannot predict the thrust force accurately and using this formula may lead to miss some physical features of the transient performance of the propulsion system. This will be analyzed here by comparing the thrust force computed by using the common formula and what calculated by pressure force integration over the solid boundaries of the flow field, in transient condition.

3 | RESULTS AND ANALYSIS

To study the unsteadiness effects on thrust force of the rocket propulsion system, the solid rocket motor which has been experimentally studied by Lee et al. [19] is investigated. The grain length is 0.264 m, the nozzle throat diameter is 0.025 m, the propellant density is 1800 kg/m³, the pressure exponent of the burning rate model is 0.43, and the flame temperature is 3000 K. In addition, the inner grain diameter (internal burning cylindrical grain) is 0.084 m and the pressure coefficient of the burning rate model is 2 mm/s. The chamber temperature and pressure are initially assumed to be 2500 K and 1 MPa, respectively. This condition is often provided by the igniter for appropriate ignition and stable burning of the whole solid propellant surface. Then, the throat diaphragm is ruptured suddenly and the engine operates. So the ignition transient is not simulated here. The reported initial operating chamber pressure (after the chamber filling phase) is about 5.3 MPa, and the thrust force is about 4 kN in this state.

To simulate this small solid rocket motor, 1200 meshes are used after grid independency studies. The pressure-time history at the head-end of the motor is computed and shown in Figure 1. This illustrates that the steady state pressure has good agreement with reported data [19]. Pressure, temperature, and Mach number distributions are also presented at steady state in Figure 2 along the motor. The nozzle exit diameter is set so that the exit pressure equals the ambient pressure at steady state which is achieved in about 0.05 s.

The thrust-time history can also be computed using the common thrust formula (F_c) and the time history of the exit mass flow rate, velocity, and pressure. This is the

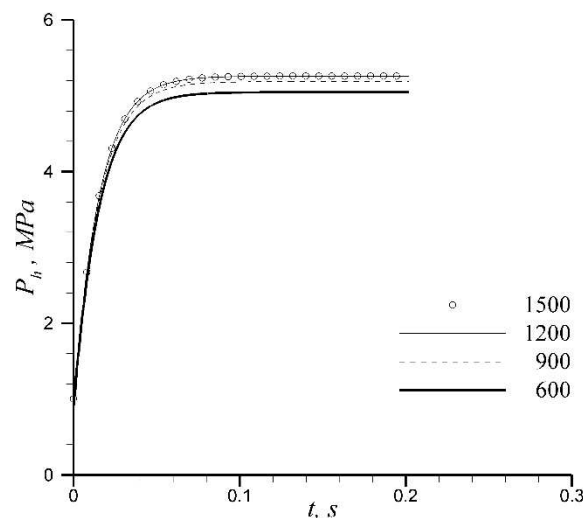


FIGURE 1 Head-end pressure time history with different grid resolutions.

method that has been always used. The result is demonstrated in Figure 3 which the steady state thrust force has good agreement again with reported data [19]. It should be mentioned that the chamber pressure and thrust force at the end of initial transient operation of this reference were 5.3 MPa and 4 kN respectively, which our results are 5.2 MPa and 4 kN respectively, shows acceptable accuracy.

Now, the thrust-time history of this solid rocket motor (SRM) is computed again without using the common formula, but with integrating the pressure force over the solid boundaries of the motor at each time step of the flow field's simulation, which is the real thrust force (F_r) applied to the propulsion system. The result (Figure 4) is

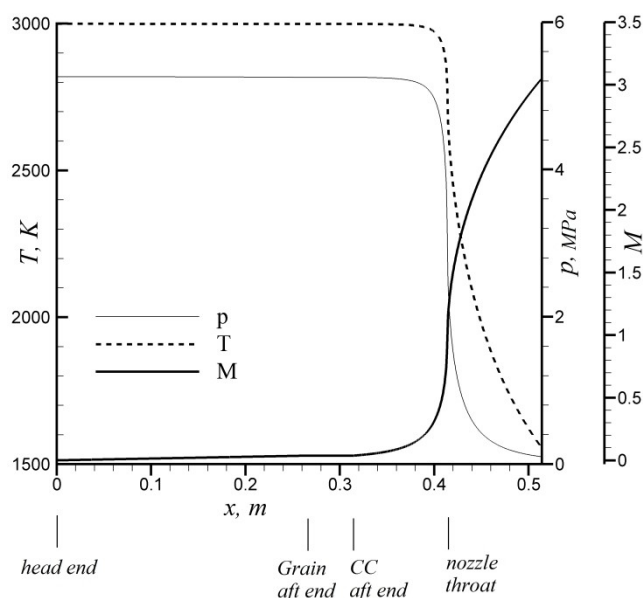


FIGURE 2 Properties distribution along motor.

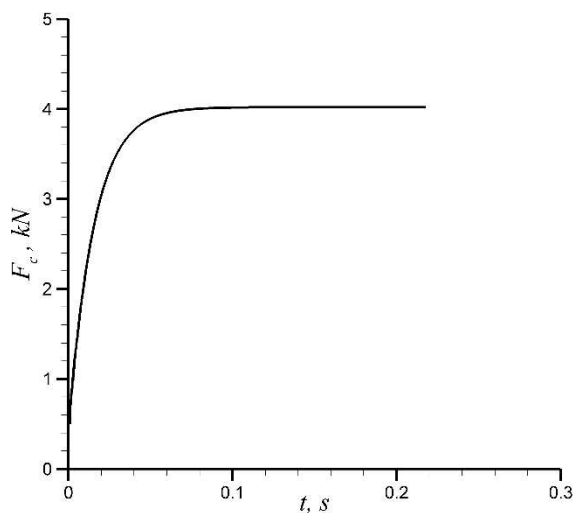


FIGURE 3 Thrust-time history based on common formula.

interesting and this is where the shortcoming of the common model appears. It is demonstrated that high amplitude thrust oscillations occur in about the first 0.02 s of the operation, which is gradually attenuated. Such oscillations may be interpreted as an error in the measurement system, but is a physical phenomenon which couldn't be observed using the common thrust model because the important assumption in derivation of this model is the steady operation of system.

At the transient phase of operation, some pressure waves sweep to the combustion chamber and convergent nozzle which cause fluctuations in pressure force on the solid boundaries. They can be seen by the pressure distribution along the combustion chamber at different time intervals, as presented in Figure 5. Such fluctuations can be created in any propulsion system at transient performance such as in throttling of the liquid fuel engines with mass flow changes. The thrust fluctuations

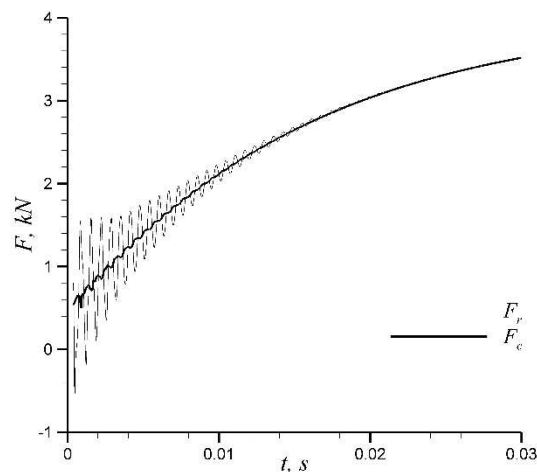


FIGURE 4 Transient thrust of the SRM.

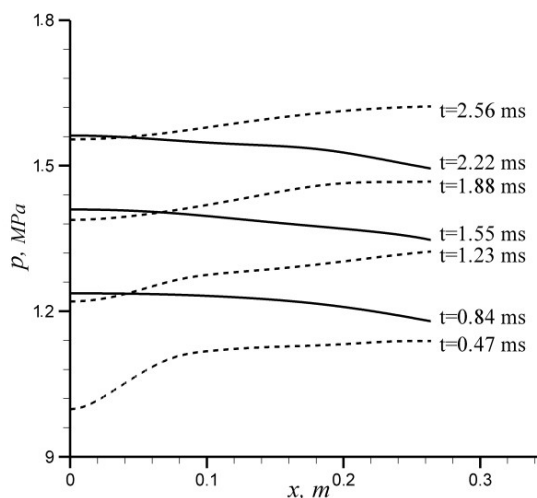


FIGURE 5 Pressure distribution along the combustion chamber at different times.

do not have a noticeable effect on the flight path of the system, but can affect the sensors or electronic equipment depending on fluctuations amplitude and frequency.

To get more insight about the amplitudes and frequencies of the thrust force fluctuations, and to estimate that for which geometries of propulsion systems these fluctuations are intense, the considered solid rocket motor is scaled in length and also in diameter, while the steady chamber pressure is kept constant, and the numerical simulations are repeated. It should be noted that when scaling the length or the diameter, the throat diameter is changed to keep the operating pressure constant. So if the length or diameter is scaled by Z factor, the throat diameter is scaled by square root of Z factor.

The results show that increasing the combustor length decreases both the amplitude and frequency of fluctuations. Also, increasing the combustor diameter

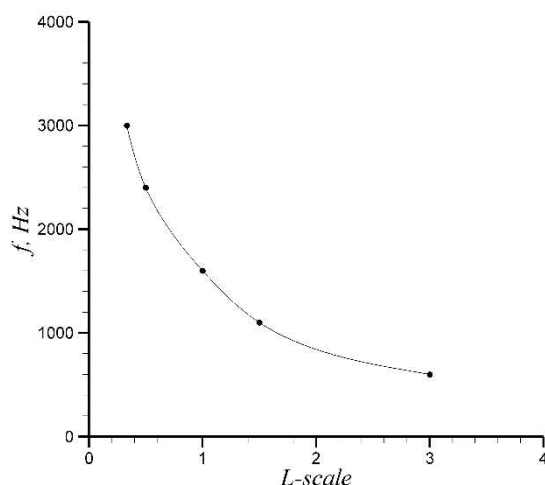


FIGURE 6 Effect of combustor length on frequency.

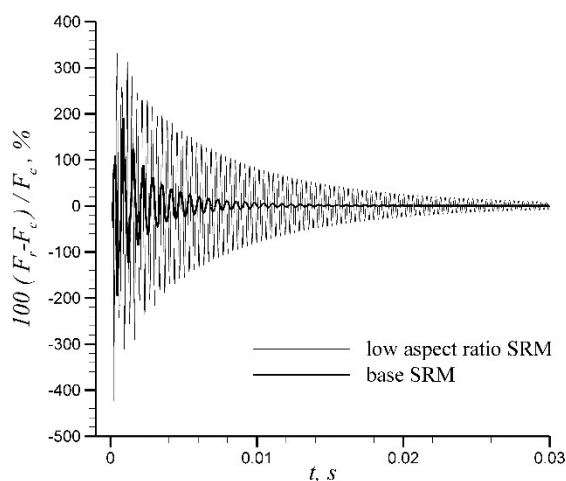


FIGURE 7 Transient thrust behavior for the base and low aspect ratio SRMs.

increases the amplitude but has no effect on frequency of fluctuation. So the frequency of the transient thrust fluctuations is just a function of the combustor length, which is presented in Figure 6 for different scaling factor of the considered SRM.

In addition, it was concluded that the amplitude of fluctuations may be augmented considerably in the propulsion systems with shorter lengths and larger diameters or indeed for low aspect ratio propulsion systems which are often used in space missions. This is shown here using the motor which its length and diameter are one-third and three times of the first considered SRM, respectively. The operating pressure is also kept constant. The transient thrust force deviations (between the real and common computations) of the scaled and the base SRMs are presented and compared in Figure 7. It is demonstrated that the amplitude of thrust fluctuations is more than 100 percent for the base SRM that is attenuated fast in less than 0.02 s as mentioned before, but in the low aspect ratio thruster, the amplitude is augmented considerably where is even more than 300 percent that is attenuated later in more than 0.03 s, and is more than 100 percent for about 0.01 s of the initial phase of operation.

The thrust force fluctuations of the propulsion system with amplitude of about 100 percent and the frequency of about 1 kHz may have harmful influences on the electronic systems of the vehicle, so it is important to compute the transient thrust accurately which can't be performed using the common way.

4 | CONCLUSIONS

Numerical simulation of an internal ballistics of the solid rocket motor is performed using quasi one-dimensional equations to study the transient thrust force accurately. This is concluded that the common thrust formula which has been derived based on steady assumption has an important shortcoming which ignores the fluctuating behavior of the real thrust force in transient operation, that may be interpreted mistakenly as an error of the measurement system. This is a physical phenomenon due to the existing moving waves in the combustion chamber and convergent nozzle in an unsteady operation of the system. The results show that the frequency of thrust fluctuations is inversely related to the combustor length and is independent to its diameter. In addition, the amplitude of thrust fluctuations is inversely related to the combustor length and is directly related to the combustor diameter. Therefore, the low aspect ratio propulsion systems such as small space thrusters are prone to stronger transient thrust fluctuations. It is

shown that the fluctuations in thrust force of the sample solid rocket motor have frequency of about 1 kHz and amplitude of more than 100 percent which are applied to the system more than 0.01 s and can be harmful for the electronic equipment of the vehicle.

DATA AVAILABILITY STATEMENT

Data may be requested via the authors.

ORCID

Amir Mahdi Tahsini  <http://orcid.org/0000-0003-0276-965X>

REFERENCES

1. A. M. Tahsini, S. A. Hosseini, *Appl. Mech. Mater.* **2014**, 598, 294–297.
2. A. M. Tahsini, K. K. N. Anbuselvan, *High Temp.* **2022**, 60, 140–142.
3. A. M. Tahsini, *Proc. Inst. Mech. Eng., Part G* **2020**, 234, 709–715.
4. S. A. Whitmore, D. Matthew, D. E. Shannon, *J. Spacecr. Rockets* **2010**, 47, 427–441.
5. C. K. Drummond, *J. Propul. Power* **1991**, 7, 465–466.
6. S. Whitmore, S. Chandler, *45th AIAA J. Propul. Conf.* **2009**, 5221.
7. P. Fabrizio, N. Souhair, S. Mini, A. Annovazzi, *AIAA Propul. Energy Forum* **2019**, 4140.
8. A. Song, N. Wang, J. Li, B. Ma, X. Chen, *Chin. J. Aeronaut.* **2020**, 33, 3189–3205.
9. E. W. Price, *Combustion Stability of Solid Propellants*, Vol. 143, AIAA, **1992**, pp. 325–361.
10. Y. Li, C. Xiong, X. Jinsheng, Z. Changsheng, O. Musa, *Acta Astronaut.* **2018**, 146, 46–65.
11. H. Tian, H. Lingfei, Y. Ruipeng, Z. Sheng, W. Pengfei, Y. Zhang, *Aerosol Sci. Technol.* **2021**, 118, 106978.
12. X. Zou, W. Ningfei, H. Lei, B. Taotao, X. Kan, *Aerosol Sci. Technol.* **2021**, 119, 107102.
13. L. Zhao, Z. Xia, L. Ma, B. Chen, Y. Duan, *Aerosol Sci. Technol.* **2022**, 130, 107945.
14. A. M. Tahsini, M. Ebrahimi, *42nd AIAA J. Propul. Conf.* **2006**, 4959.
15. P. Roe, *J. Comput. Phys.* **1981**, 43, 357–372.
16. A. M. Tahsini, M. Farshchi, *J. Propul. Power* **2007**, 23, 1142–1142.
17. A. M. Tahsini, *45th AIAA Aero Sci. Meeting* **2007**, 1419.
18. A. M. Tahsini, *45th AIAA Aero Sci. Meeting* **2007**, 777.
19. S. Lee, S. W. Baek, K. Kim, *J. Propul. Power* **2010**, 26, 980–986.

How to cite this article: A. Zanjani, A. M. Tahsini, *Propellants, Explos., Pyrotech.* **2023**, 48, e202300101. <https://doi.org/10.1002/prep.202300101>